Biophys. Struct. Mechanism 5, 75–90 (1979)

Biophysics of Structure and Mechanism
© Springer-Verlag 1979

Complex Formation of Acridine Orange with Single-Stranded Polyriboadenylic Acid and 5′-AMP: Cooperative Binding and Intercalation Between Bases

V. von Tscharner and G. Schwarz

Department of Biophysical Chemistry, Biocenter of the University of Basel, Klingelbergstraße 70, CH-4056 Basel, Switzerland

Abstract. The binding of acridine orange to single-stranded polyribonucleic acid at low polymer to dye ratios exhibits cooperative behavior of the kind observed with other simple polyanions. It is thus attributed to electrostatic interaction between polymer and stacked dye molecules. At higher polymer to dye ratios, however, distinct deviations from the predictions of the basic theory occur. These are interpreted by additional non-cooperative binding of acridine orange to the bases of the polymer subunits owing to dye-base stacking. This effect is studied also with 5′-AMP monomers where it likewise leads to complex formation. Both systems are investigated experimentally by means of the changes produced in the dye spectrum. Based on quantitative analyses the equilibrium constants of both systems are evaluated and discussed. They indicate a sandwich-type of intercalation of dye between two bases of the single-stranded polymer.

Key words: Acridine orange – Polyriboadenylic acid – Intercalation – Cooperative binding – Stacking interaction.

Introduction

The binding of acridine orange (AO) and other acridine dyes to biopolymers plays an essential role in a number of phenomena in molecular biology and genetics. Tumor destruction due to AO photoactivation by argon laser has been studied (Tomson, 1976). Another application of AO is the elimination of episomes from bacteria (Halm and Ciak, 1971). Early cell damage could be detected by AO staining to the cell, whereby the AO binds to the DNA (Söderström et al., 1977). Different binding modes of AO to double-stranded DNA and single-stranded RNA were used for staining of unfixed cells (Taraganos et al., 1977). The circular dichroism of AO bound to poly(L-glutamic acid) (Imae and Ikeda, 1976) or other biopolymers show that one can detect the structural behavior of the polymer. The binding of AO to DNA can be investigated by viscometry and dynamic birefringence (Moroshkina et al., 1976).

0340-1057/79/0005/0075/$ 03.20

The main action in binding AO to a charged linear biopolymer consists of electrostatically fixed dye molecules stabilized by dye-dye stacking. The process can be described by a fundamental cooperative approach (Schwarz, 1970) based on the linear Ising model (Ising, 1925). Assuming that all binding sites along the chain are equivalent the binding of the first AO molecule is taken to be relatively difficult because it is only due to electrostatic interactions. This nucleation is followed by the binding of AO to binding sites just adjacent to a bound AO, a process which is expected to be favored by stacking interactions (growth). The cooperative binding consists of nucleation and growth. The theory takes into consideration only the nearest neighbor interactions. Effects due to the ends of the polymer can be neglected because the average length of stacks is small compared with the polymer length. The ratio of the binding constant for the nucleation, K^*, to the binding constant for growth, K, is called the cooperativity parameter, σ. For the cooperative binding of a ligand to a polymer σ can be measured best at large polymer to dye ratios, p. With increasing p the stacks become shorter and shorter and at very large p only singly-bound ligands are present. This description was found to be very suitable for AO binding to poly-glutamic acid and other poly-anions (Schwarz and Balthasar, 1970; West et al., 1977; Menter et al., 1977). The calculated curves could be made to fit very well the binding data obtained from absorption measurements.

In DNA and polynucleotide a second binding process often occurs and is due to dye-base stacking. The AO has about the same size as the nuclear bases and is believed to intercalate into the double-stranded DNA (Lerman, 1963). In single-stranded DNA a partial intercalation model has been proposed by Pritchard et al. (1966). "The basis of the model is that acridine does not interact with a hydrogen bonded base pair, but rather that the interaction occurs between an acridine and two adjacent bases on the same polynucleotide chain." Both the intercalated and the partial intercalated AO will compensate the charge of the phosphate group at the binding site. Intercalation and cooperative binding require the same charges of the polymer for fixation and therefore the two binding modes will exclude each other.

Dourlent and Hélène (1971) investigated the binding of proflavin to single-stranded poly(A). They found outside binding and dye-base stacking occuring. They analyzed the absorption data assuming both processes to be independent of one another with the basic cooperative model. The outside binding was positively cooperative and the dye-base stacking anti-cooperative. They could see that the binding sites are not independent.

AO binding to single-stranded poly(A) proved to be a suitable system for studying the effects of partial intercalation in connection with cooperative binding. AO molecules are known to stack very strongly with each other, forming dimers in dilute solution even for concentrations smaller than 10^{-4} M and have great cooperativity when binding to a polymer. Usually it is believed that acridine dyes intercalate into DNA, but little is known about the thermodynamic parameters in the case of intercalation into single-stranded nucleic acids. An AO bound to the poly(A) by nucleation can intercalate by twisting around the backbone and stacking with one or two bases. The aim of measuring the cooperativity parameter at large p-values with the basic model failed. It will

be shown that from the shape and the position of the absorption curve, as depicted in Figure 5, one can determine the ratio of nucleated to intercalated AO. The competition postulated for the two binding modes involved a very specific binding behavior. With decreasing p (increasing the dye- or decreasing the polymer concentration) a sudden appearance of stacks can be registered.

There is no proof that intercalated AO stacks to both adjacent bases, it could as well bind to only one adenine ring. In the first case the intercalation would introduce some rigidity into a poly(A) coil, changing its conformation, whereas in the second case no major conformational change would be expected. Binding studies of AO to 5′-AMP provided the evidence that stacking occurs to both adjacent bases.

Material and Methods

Poly(A) from Sigma and 5′-AMP from Serva were used without further purification. The concentrations have been measured spectrophotometrically using molar absorption coefficients $\varepsilon(\lambda)$. For poly(A) at 28° C, pH 7: $\varepsilon^{257\,\mathrm{nm}} = 10.5 \cdot 10^3\ \mathrm{M}^{-1}\ \mathrm{cm}^{-1}$ (Singer et al., 1962; Blake and Fresco, 1973); for 5′-AMP at 20° C, pH 2.0 $\varepsilon^{260\,\mathrm{nm}} = 14.2 \cdot 10^3\ \mathrm{M}^{-1}\ \mathrm{cm}^{-1}$. Unless indicated otherwise all measurements were performed at 20° C and with 50 mM NaCl added to all solutions. Solutions with single-stranded poly(A) contained 5 mM phosphate buffer at pH 7, whereas solutions with 5′-AMP contained 5 mM Tris buffer at pH 8.5.

AO from Fluka, Switzerland, has been purified by the method described elsewhere (Robinson et al., 1973). For further purification about 1.5 g of AO was dissolved in 1 l of water. An equal amount of ether was added. Solid KOH was added until the AO redissolved completely. The mixture was then allowed to stand for 30 min. The ether from the clear yellow supernatant was evaporated in a vacuum desiccator. The remaining dye was analyzed by elemental analysis and showed to be pure within 98%.

AO was adsorbed very much by glass and metals. Therefore stock solutions were prepared in plastic bottles in large amounts in order to reduce the surface to volume ratio. All contact with glass and metal was avoided and the solutions were kept in the dark. In order to further reduce adsorbance, synthetic cells from Sarstedt were used for the measurements. These cells adsorb only about 1% of the free dye on their surface. Adsorption measurements were performed on a Cary 1605 and on a Cary 118 double beam spectrophotometer. All spectra are normalized by dividing the absorption by the total dye concentration c_A^0 and the cell length.

Attempts to perform binding studies of AO to poly(A) by the filtration method (Menter et al., 1977) were not successful. Two cuvets filled with 3 ml of $2.5 \cdot 10^{-5}$ M AO were put into the Cary 1605. 256 mm^2 of nucleopor filter was added and one could see that 20% of the dye adsorbed within 1.5 h. This means that at least $5 \cdot 10^{-9}$ M AO binds per cm^2 and this is too much to be accepted.

AO with concentrations below $5 \cdot 10^{-5}$ M is believed to form only dimers, whereas at higher concentrations larger aggregates will be formed (Robinson

et al., 1973; Zanker, 1952; Lamm and Neville, 1965; Kurucsev and Strauss, 1970). We will only take into account dimerization. The wavelength for the isosbestic point $\lambda_i = 470$ nm and the corresponding adsorption coefficient $\varepsilon^{470} = 43{,}300 \pm 800\ M^{-1}\ cm^{-1}$ have been measured. Most published values are smaller: $41{,}000\ M^{-1}\ cm^{-1}$ (Zanker, 1952), $43{,}000\ M^{-1}\ cm^{-1}$ (Lamm and Neville, 1965), $42{,}000\ M^{-1}\ cm^{-1}$ (Armstrong et al., 1970), $39{,}000\ M^{-1}\ cm^{-1}$ (Kurucsev and Strauss, 1970). The concentrations, c_A^0, of all further solutions were then calculated from the adsorption A^{470}

$$c_A^0 = \frac{A^{470}}{\varepsilon^{470}} . \tag{1}$$

For the formation of AO dimers the equilibrium constant K_D and the concentration of the monomeric AO is characterized by the following equations:

$$K_D = (c_A^0 - c_M)/(2\, c_M^2) , \tag{2}$$

$$c_M = \gamma_M c_A^0 , \tag{3}$$

where

$$\gamma_M = (\varepsilon - \varepsilon_D)/(\varepsilon_M - \varepsilon_D) .$$

ε_M and ε_D are the absorption coefficients of the monomeric and dimeric AO. Usually one uses the absorption coefficients at 492 nm for the determination of c_M.

ε_M, ε_D and K_D were determined by a least square fit of these parameters to the absorption at 492 nm for different c_A^0, giving

$$\varepsilon_M^{492} = (65{,}800 \pm 1{,}000)\ M^{-1}\ cm^{-1} \text{ and } \varepsilon_D^{492} = (1{,}000^{+\,2{,}000}_{-\,1{,}000})\ M^{-1}\ cm^{-1} .$$

K_D is dependent on the ionic strength and can be determined by absorption measurements at 470 and 492 nm by Eqs. (1), (3), and (2) ($K_D = 11{,}200\ M^{-1}$ without salt and $K_D = 14{,}500\ M^{-1}$ with 50 mM sodium chloride at pH 7).

Assuming ε_M and ε_D to be independent of temperature the complete spectra can be calculated from measurements at two different temperatures (Fig. 1). From a van't Hoff plot $\Delta H^0 = -30.4 \cdot 10^3\ J\ mol^{-1}$ and $\Delta S^0 = 23.6\ J\ mol^{-1}\ K^{-1}$ were obtained.

Theory Connecting the Two Binding Modes of AO on poly(A)

Cooperative binding and dye-base stacking were mainly treated as independent binding modes. In polynucleotides both processes are well known. The following theoretical modification of the basic cooperative model (Schwarz, 1970) had to be introduced because neither binding process could explain the measurements when both cooperative binding and dye-base stacking occurred simultaneously. A binding site on a polynucleotide is provided by the negatively charged phos-

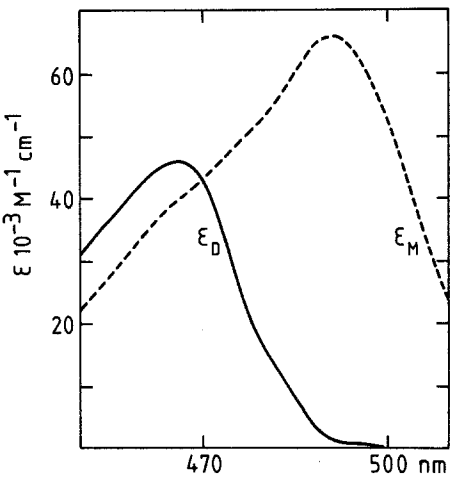

Fig. 1. The absorption coefficient of monomeric (- - -) and dimeric (——) AO at pH 7 (see text)

phate group. A binding site occupied by either binding mode will no longer be available for the other one. The two binding modes mutually exclude each other. AO bound by nucleation to the outside (N) can by dye-base stacking change its binding mode to a partial intercalated one (I).

$$N \rightleftharpoons I, \qquad K' = c_I/c_N, \tag{4}$$

c_I and c_N are the molar concentrations of the intercalated and nucleated AO. At this stage no assumption is made about stacking of the dye to one or to both adjacent bases.

If c_I is small compared to that of the binding sites the growth of AO stacks (S) will not be hindered by the intercalated AO. The mean distance between intercalated AO will be long compared to the mean length of stacks. We further assume no change of the binding mode can occur within a stack of AO molecules because of the stabilizing energy due to the dye-dye stacking. This is the simplest model that we could imagine to combine the two binding modes and for extreme conditions such as a very large K' value it would be necessary to introduce a more sophisticated model.

If we now derive the formulas used for the model coupling the cooperative binding with intercalation, the corresponding formulas for the basic cooperative model can be obtained by setting $K' = 0$ which means $c_I = 0$.

For the mathematical treatment of the model we extend the method described earlier (Schwarz, 1970). If the concentrations of the different species present are known, the absorption A can be calculated from the sum of the products of the concentrations with their respective absorption coefficients. The cell length is always 1 cm if not otherwise indicated. All stacked AO molecules even those at the end of a stack are assumed to have the same absorption coefficient ε_S.

$$A = \varepsilon_M c_M + 2\,\varepsilon_D c_D + \varepsilon_N c_N + \varepsilon_S c_S + \varepsilon_I c_I\,. \tag{5}$$

(M: monomeric, D: dimeric, N: nucleated, S: stacked and bound, I: intercalated)

The fraction θ of cooperatively bound AO is given by

$$\theta = (c_N + c_S)/g\, c_p\,, \tag{6}$$

where $g\, c_p$ is the concentration of binding sites with $c_p = p\, c_A^0$. θ can be calculated from statistical thermodynamics (Schwarz, 1970):

$$\theta = 0.5\{1 - (1 - s)\,[(1 - s)^2 + 4\,\sigma s]^{-1/2}\}\,, \tag{7}$$

where K is the binding constant for growth and $s = Kc_M$, K^+ is the binding constant for nucleation and $\sigma = K^+/K$ is the cooperativity parameter.

Taking into account the mass conservation of dye, it follows

$$\theta = (c_A^0 - c_M - 2\,K_D c_M^2 - c_I)/g\, c_p\,. \tag{8}$$

Thereby we assume $c_I \ll g\, c_p$ and we ignore the fact that the intercalated AO will reduce the number of binding sites. For the monomeric bound dye the concentration is also calculated from statistical thermodynamics (Schwarz, 1970).

$$c_N = g\, c_p \sigma s(1 - \theta)/\lambda_0^2\,, \tag{9}$$

$$\lambda_0 = (1 + s)/2 + \{(1 - s)^2 + 4\,\sigma s\}^{1/2}\,.$$

Introducing c_N and $c_I = K' c_N$ into Eq. (8) it is found that

$$(c_A^0 - c_M - 2\,K_D c_M^2)/g\, p c_A^0 - K'\sigma K c_M/\lambda_0^2 = \theta\,(1 - K'\sigma K c_M/\lambda_0^2)\,. \tag{10}$$

With insertion of θ from Eq. (7), the only variable in Eq. (10) is c_M. An iterative procedure on a calculator must be used to solve Eq. (10) for c_M.

From $g\, p$ and the total dye concentration c_A^0 with a given set of parameters (K', K, σ) all expected concentrations c_M, c_N, c_I, and c_S can be evaluated from Eqs. (10), (7), (9), (8), and (6). The absorption is obtained by introducing the known concentrations into Eq. (5). If we assume $\varepsilon_N = \varepsilon_M$ we will have two more parameters ε_S and ε_I to choose. A theoretical curve can be fitted to the experimental values by variation of the parameters (K', K, σ, ε_I, ε_S). The constraints for the model calculations were $c_I \ll g\, c_p$ and the polymer chains must be long. All theoretical curves in the different plots are calculated by this set of equations even if the parameter has been determined by a simplified formula.

Results and Discussion

A. AO Binding to Poly(A)

We focus now our attention on the model without intercalation and determine the parameters ε_S, g, K, following the method described elsewhere (Schwarz and Balthasar, 1970). For strong cooperativity $\sigma^{1/2} \ll 1$ and constant p, from

Eqs. (7) and (5) the following equation can be derived for the extinction coefficient

$$A/c_A^0 = \varepsilon = \varepsilon_S + (\varepsilon_M - \varepsilon_S)\frac{s_0}{K}(c_A^0)^{-1}, \tag{11}$$

with

$$s_0 = 1 - (1 - 2\,\theta)(\sigma g\, p)^{1/2}(1 - \theta)^{-1/2}.$$

A plot of ε versus $(c_A^0)^{-1}$ should show a straight line when c_A^0 is large (Fig. 2). $s_0 \approx 1$ is then constant because $\theta \approx 1/g\,p$. The intercept is $\varepsilon_S^{492} = 16{,}000 \pm 500\ \mathrm{M^{-1}\ cm^{-1}}$ ($\varepsilon_S^{470} = 28{,}500 \pm 1{,}000\ \mathrm{M^{-1}\ cm^{-1}}$, $\varepsilon_S^{462} = 33{,}500 \pm 1{,}500\ \mathrm{M^{-1}\ cm^{-1}}$). When σ is determined, s_0 can be calculated more precisely and K deduced from the slope of the curve (with $\sigma = 1{,}000^{-1}$ at $p = 3$, $s_0 = 0.97$; $K = 5 \cdot 10^6\ \mathrm{M^{-1}} \pm 10\%$). Using $s_0 = 1$, we should have had an error of only 3%.

From Eq. (6) we find the relative amount of dye which is not bound in the cooperative mode, γ_A^*. γ_A^* represents the sum of free and intercalated relative dye amounts.

$$\gamma_A^* = 1 - \theta g\, p\,. \tag{12}$$

For very small p we have $\theta \approx 1$ and the slope of a plot of γ_A^* versus p will be g (Fig. 3). The measured data could be fitted with $\sigma = 10^{-3}$, $K = 5 \cdot 10^6\ \mathrm{M^{-1}}$ and yield $g = 1.03 \pm 5\%$. Therefore we may set $g = 1$, which means every phosphate group is available as a binding site. To determine the cooperativity parameter σ it is best to measure the absorption coefficient ε at large p, where the stacks get shorter and more dye becomes singly attached. Assuming $\varepsilon_N = \varepsilon_M$, an assumption which proved to be correct for the binding of AO to poly-glutamic acid (Schwarz and Balthasar, 1970), a plot of ε versus $\log p$ can be calculated (Fig. 4). The whole curve is shifted parallel to the p-axis when σ is changed. The limiting value of ε at very large p could be adjusted by altering ε_N but the shape of the curve is very little influenced. The absorption measurements at $\lambda = 492$ nm and $\lambda = 462$ nm are depicted in Figure 5. These data cannot be fitted with the basic model. But for instance, for AO binding to poly-glutamic acid the shape of the model curve fits the measured data and suggests that the model is correct. This behavior forced us to look in more detail at the system and we will now analyze the influence of intercalation.

We first look at Eq. (11) and we realize that if $\theta < 1/2$, s_0 will be larger with a lower σ. If $p \approx 1$ and $\theta \approx 1/g\,p$, no intercalation can occur because all binding sites are occupied. From the linear region of Figure 2 we can as before determine K and ε_S. A deviation from predictions of the simple model will only occur at low c_A^0. The same argument holds for the slope at small p in Figure 3, where $\theta \approx 1$ and no intercalation occurs. Therefore the factor g stays the same as before but from this plot K should not be determined by the usual method because at a larger p we may have intercalated dyes. At large p a significant consequent influence can be observed. In Figure 4 the extinction is calculated for different σ at $\lambda = 492$ nm keeping $\sigma K' = 10^{-3}$ constant and using $\varepsilon_M = \varepsilon_N$ and $\varepsilon_I = 46{,}000\ \mathrm{M^{-1}\ cm^{-1}}$. The position of the curve is now determined by $\sigma K'$ and with increasing K' it becomes steeper and steeper reaching a limiting

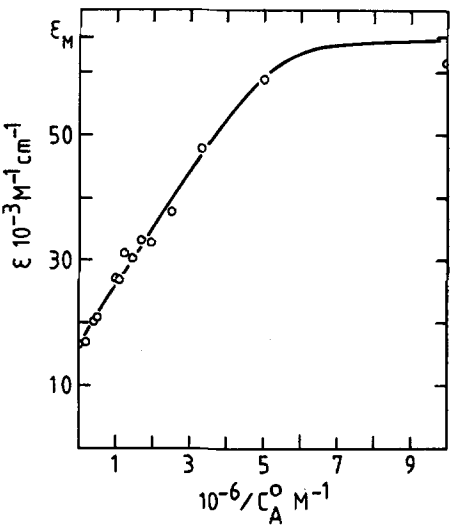

Fig. 2. The absorption coefficient (492 nm) of AO at constant $p = 3$ as a function of reciprocal total dye concentration

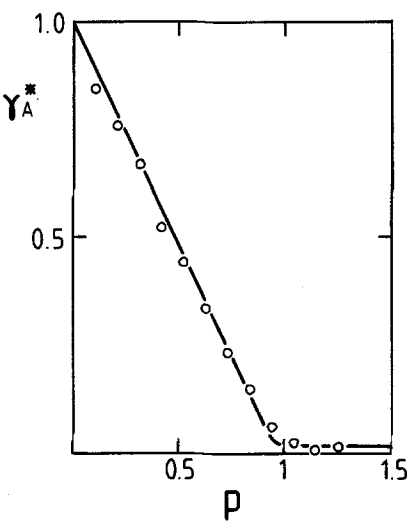

Fig. 3. The relative amount γ_A^* of not bound AO as a function of the polymer to dye ratio ($c_A^0 = 1.43 \cdot 10^{-5}$ M, pH = 7 without NaCl)

slope. If K' is small more nucleated AO is present and stacks will more easily form than with a large K'. The absorption measurements at $c_p = 1.25 \cdot 10^{-3}$ M and $\lambda = 492$ nm as a function of $\log p$ depicted in Figure 5 can be fitted with the parameters $K = 5 \cdot 10^6$ M^{-1}; $K' = 10^3$, $\sigma = 10^{-6}$ ($\sigma K' = 10^{-3}$); $g = 1$; $K_D = 14{,}500$ M^{-1}; $\varepsilon_M = \varepsilon_N = 65{,}800$ M^{-1} cm^{-1}; $\varepsilon_D = 1{,}000$ M^{-1} cm^{-1}; $\varepsilon_S = 16{,}000$ M^{-1} cm^{-1} and $\varepsilon_I = 46{,}000$ M^{-1} cm^{-1}. With these values we nearly reached the limiting slope. Therefore K' and σ can only be estimated ($K' \gtrsim 100$; $\sigma \lesssim 10^{-5}$) but $\sigma K' = 10^{-3}$ has little error. $\sigma = 10^{-5}$ would be at the upper limit of the values usually measured with AO (Moroshkina et al., 1976; Eggimann, 1974). With another wavelength the measurements could be fitted by approximating only ε_I, keeping the binding constants fixed (Fig 5). This is a necessary

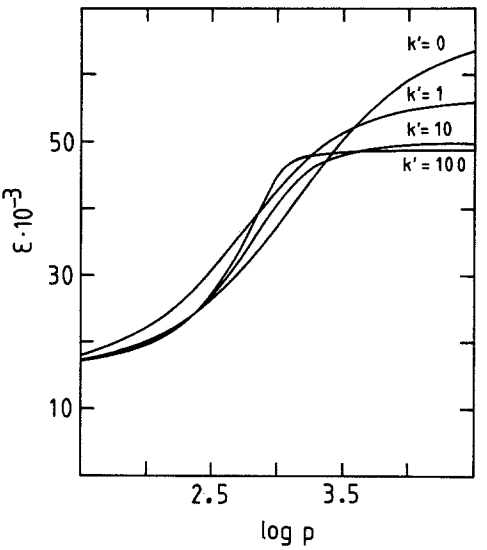

Fig. 4. Theoretically calculated adsorption coefficients (same parameters as in Figure 5 and given in the text)

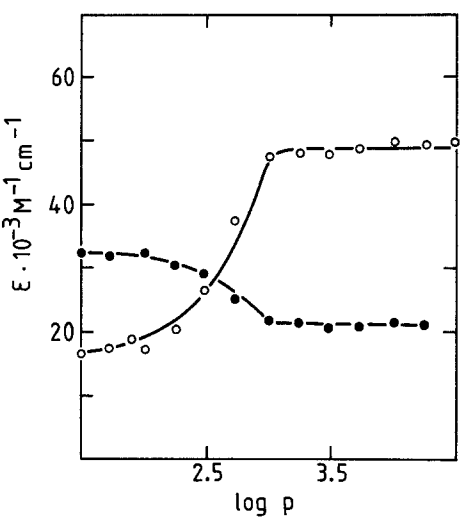

Fig. 5. Measured absorption coefficients at 492 nm (○) and at 462 nm (●) for large p-values. The lines are calculated from the theoretical model of cooperativity and intercalation ($c_p = 1.25 \cdot 10^{-3}$ M and parameters given in the text)

consequence of the model and a strong support for its validity. With a Farrand spectrofluorometer Mark I we could show that the fluorescence emission at 530 nm (excitation at 470 nm) in the case of intercalated AO is larger than emission by the free dye. The emission of stacked dyes is totally quenched at 530 nm.

With these parameters the measured data at low p-values for $\lambda = 492$ nm could be as well fitted as by the simple model. Measurements at low p and at wavelengths differing from 492 nm could not be fitted with these models. Probably some structural transformation of the single-stranded helix could occur followed by a rearrangement of the stacks. The stacks have a maximum in their spectrum at $\lambda = 460$ nm and the extinction coefficient at $\lambda = 492$ nm is small. Therefore

no detectable change of the stacks would be seen in the absorption at $\lambda = 492$ nm. In the region of extremely large p the spectrum of the intercalated AO is seen to be red-shifted and to have a maximum at $\lambda = 502$ nm ($\varepsilon_I^{502} = 60 \cdot 10^3$ M^{-1} $cm^{-1} \pm 5\%$). We would like to know more about the intercalated AO. Therefore we first have to investigate the base-dye stacking in a simpler case to see what structure may appear. The stacking to 5′-AMP, the monomeric unit of poly(A), will be useful and its properties may be applicable to the intercalation of AO into poly(A).

A very much smaller K' is reported for proflavin binding to poly(A) (Dourlent and Hélène, 1971). The main experimental difficulty besides the adsorption of AO was the precipitation which often occurred at small p, $p \approx 1$. The main advantage for the precise measurements were the Sarstedt cuvets which did not adsorb AO.

B. AO Interacting with 5′-AMP

From the similarly red-shifted spectra of a solution of AO and 5′-AMP and one of AO and poly(A) at large p, it can be concluded that the binding is similar to that of the dye-base interaction in poly(A). A simple explanation by assuming one AO stacking to one 5′-AMP failed and no binding constant could be determined. We have to look in more detail at this binding and additional complexity has to be considered.

As long as the intramolecular equilibrium between the different conformations of 5′-AMP (Bloomfield et al., 1974; Evans and Sarma, 1974) is not changed, one can consider 5′-AMP to be a uniform species as far as binding is concerned. The pK 6.2 refers to the second protonation of the phosphate group. The system is only well defined if one works at a pH above 6.2, where 5′-AMP has two negative charges. The pH should be smaller than the pK 10.3 of the AO protonation. Therefore we choose a pH 8.5 as a working point. Like AO, 5′-AMP also can form dimers or higher aggregates (Lehninger, 1970), but this effect can still be neglected at our concentrations of 5′-AMP (this species to be denoted as B). Nevertheless these appear to suffice for a formation of a complex AB caused by stacking interaction between A (i.e., acridine orange) and B. Further stacking between the A in AB and either A or B in their monomer states may then result in appreciable amounts of AAB or BAB complexes, respectively. On the other hand, we need not take into account $AB + A \rightarrow ABA$ or $AB + B \rightarrow ABB$ since $c_{AB} < c_A^0 \ll c_B$.

An experimental method and its mathematical analysis to decide about the actual presence of both possible higher complexes will be discussed in the appendix. The results show that beside AB practically only the AAB form occurs. The two respective binding equilibria are described according to

$$A + B \underset{K_{AB}}{\rightleftharpoons} AB\,, \qquad K_{AB} = \frac{c_{AB}}{c_A c_B}\,,$$

$$A + AB \underset{K_A}{\rightleftharpoons} AAB\,, \qquad K_A = \frac{c_{AAB}}{c_{AB} c_A}\,.$$

We got the following equilibrium constants and absorption coefficients:

$$K_{AB} = 100 \pm 5\ \mathrm{M}^{-1}, \qquad K_A = 8.2 \cdot 10^3\ \mathrm{M}^{-1},$$

$$\varepsilon_{AB}^{492} = 5.5 \cdot 10^4\ \mathrm{M}^{-1}\ \mathrm{cm}^{-1}, \qquad \varepsilon_{AAB}^{492} < 5{,}000\ \mathrm{M}^{-1}\ \mathrm{cm}^{-1}.$$

Conclusions

A comparison of AO binding to 5′-AMP and poly(A) reveals that AO stacks to both adjacent bases when intercalating into a single-stranded poly(A). The binding constant for fixing an AO molecule from solution to the dye-base stacked mode on poly(A) is $K\sigma K' = 5{,}000\ \mathrm{M}^{-1}$. The precision is dependent on $\sigma K'$ which can be determined very exactly. $K\sigma K'$ can be compared with $K_{AB} = 100\,\mathrm{M}^{-1}$, the binding constant for fixing an AO to 5′-AMP. In both cases the electric charges are compensated and dye-base stacking occurs. The fact that AO has a larger affinity to poly(A) than to 5′-AMP can only be accounted for by a further stacking interaction. This shows that both adjacent adenine bases are stacking to the intercalated AO. The result also implies a certain change in the poly(A) conformation.

In the coiled part of poly(A) the two adenine bases stacking to AO will be forced to lie on the same side of the backbone and to be parallel with the AO. More rigidity will be introduced into the poly(A) strand. Intercalation in the helical part will, as in double-stranded DNA, be followed by a local untwisting of the helical segment. Thereby the helical part will be elongated. In single-stranded poly(A) one has coiled and helical parts but we could not decide which part is preferentially used for intercalation. As $g = 1$ the whole poly(A) strand is available for cooperative binding. This implies that the adenine bases must lie opposite the AO stacks. A certain conformational change is therefore induced by the cooperative binding which will favor the adenine-adenine stacking and thus the forming of helical parts.

We have a similar intercalation of AO into poly(A) as in other polynucleotides and DNA. Thus we can discuss the more general aspects of the model coupling the intercalation with the cooperative binding which is due to the competition at the same binding sites. Intercalation occurs at large p (low concentration of dye). Stacks will be formed when p is decreased but in combination with intercalated AO this formation can be realized within a much smaller concentration range than one would expect without intercalation. The forming of stacks is a very sudden process especially if K' is large. The p-value for this sudden formation of stacks will be altered by K'. K' is, for instance, dependent on the G-C content of DNA. With the same σ for the outside binding determined by the backbone structure, however, intercalation can occur in one part of the DNA and mainly cooperative binding in another. The part with lower K'-value will have $\sigma K'$ smaller than the other and therefore stacks will be stable up to a larger p-value. The part with a larger K' will then be in a stage with only intercalated AO molecules, whereas the other still has stacks. This behavior could explain the possibility of elimination of episomes from bacteria (Halm

and Ciak, 1971) or the possibility of staining RNA and DNA in a different way (Taraganos et al., 1977). The model also applies to other dyes and drugs stacking and intercalating to a linear charged biopolymer.

The fluorescent aspects are not yet completely analyzed but the main properties for AO are the quenching of cooperatively bound dye fluorescence and the increase in fluorescence for intercalated AO (Schreiber and Daune, 1974).

Acknowledgement. This work was supported by grants of the Swiss National Foundation (Kredit No. 3.015.73 and No. 3.487.75 des Schweizerischen Nationalfonds zur Förderung der wissenschaftlichen Forschung).

Appendix

To decide whether we have an AAB or a BAB complex forming we must consider the following equilibria:

Equilibrium	Equilibrium constant	Absorption coefficient of the product
$A + A \rightleftharpoons AA$	K_D	ε_D,
$A + B \rightleftharpoons AB$	K_{AB}	ε_{AB},
$BA + B \rightleftharpoons BAB$	K_B	ε_B,
$A + AB \rightleftharpoons AAB$	K_A	ε_A.

(A1)

The absorption, including the known AO dimerization, can be calculated as follows:

$$A = \varepsilon c_A^0 = c_A \varepsilon_M + 2\, K_D c_A^2 \varepsilon_D + c_{AB} \varepsilon_{AB} + c_{BAB} \varepsilon_B + 2\, c_{AAB} \varepsilon_A \,. \tag{A2}$$

The equation für mass conservation is:

$$c_A^0 = c_A + 2\, K_D c_A^2 + c_{AB} + c_{BAB} + 2\, c_{AAB} \,. \tag{A3}$$

We look only at solutions where the weighed-in-concentration of 5′-AMP c_B is much larger than c_A^0. For calculation, however, we make no further difference between free and weighed-in-concentration of 5′-AMP. The following substitutions will facilitate the mathematics:

$$\begin{aligned} \psi &= (1 + K_{AB} c_B + K_{AB} K_B c_B^2) \,, \\ \phi &= (\varepsilon_M + K_{AB} c_B \varepsilon_{AB} + K_{AB} K_B c_B^2 \varepsilon_B) \,, \\ R &= c_B K_{AB} K_A / K_D \,, \\ Q &= (1 + R\varepsilon_A/\varepsilon_D)/(1 + R) \,, \\ \alpha &= (\phi - \varepsilon_D \psi Q) \,. \end{aligned} \tag{A4}$$

Eqs. (A2) and (A3) are rewritten as:

$$A = c_A \phi + 2\, K_D c_A^2 (\varepsilon_D + R\varepsilon_A) \,, \tag{A5}$$

$$c_A^0 = c_A \psi + 2\, K_D c_A^2 (1 + R) \,. \tag{A6}$$

This form clearly shows the c_A dependence, if c_B is constant. With c_B constant, ϕ, ψ, and R are also constant. The Eqs. (A5) and (A6) are suitable for the computer. To discuss the model, plots of the measurements should be produced, which can easily check the different possible equilibra.

Therefore we further transform Eqs. (A5) and (A6):

$$2\, K_D c_A^2 = (c_A^0 - c_A \psi)/(1 + R) \,, \tag{A7}$$

$$c_A = (\varepsilon - Q\varepsilon_D) c_A^0 / \alpha \,. \tag{A8}$$

Introducing c_A from (11) into (A6) we obtain the fundamental equation:

$$\psi/\alpha + 2\,K_D c_A^0(1+R)(\varepsilon - \varepsilon_D Q)/\alpha = (\varepsilon - \varepsilon_D Q)^{-1}\,. \tag{A9}$$

For the discussion, it is useful to make the approximation $Q \approx 1$.

$$(\varepsilon - \varepsilon_D Q)^{-1} \approx (\varepsilon - \varepsilon_D)^{-1} + (Q-1)\varepsilon_D/(\varepsilon - \varepsilon_D)^2 \tag{A10}$$

and to introduce it into (A9).

$$\begin{aligned}\psi/\alpha + 2\,K_D c_A^0(1+R)(\varepsilon - \varepsilon_D)\alpha^2 \\ + \{2\,K_D c_A^0(1+R)\varepsilon_D/\alpha + \varepsilon_D/(\varepsilon - \varepsilon)^2\}(1-Q) = (\varepsilon - \varepsilon_D)^{-1}\,.\end{aligned} \tag{A11}$$

This equation can now be discussed for the different models.

For the case that only BAB would be formed we have $K_A = 0\ \mathrm{M}^{-1}$, $R = 0$, and $Q = 1$. Eq. (A11) reduces to

$$\psi/\alpha + 2\,K_D c_A^0(\varepsilon - \varepsilon_D)/\alpha^2 = (\varepsilon - \varepsilon_D)^{-1}\,. \tag{A12}$$

A plot of $(\varepsilon - \varepsilon_D)^{-1}$ as a function of $c_A^0(\varepsilon - \varepsilon_D)$, leaving c_B constant, should show a straight line (Fig. 6). The intercept I and the slope S are:

$$I = \psi/\alpha\,; \quad S = 2\,K_D/\alpha^2\,. \tag{A13}$$

Forming the ratio $I/S^{1/2}$, α is eliminated

$$I/S^{1/2} = \psi/(2\,K_D)^{1/2}\,. \tag{A14}$$

A plot of $I/S^{1/2}$ as a function of c_B should show a straight line, but not as measured a curve with decreasing slope (Fig. 7). With increasing c_B one should get quadratic terms in ψ and the slope should increase.

Therefore the BAB-complex will not form up to $c_B = 2 \cdot 10^{-2}$ M. But the decrease in slope in Figure 7 tells us that there is more than just an AB-complex forming.

For the case that only AAB would be formed we have $K_B = 0\ \mathrm{M}^{-1}$; $R \neq 0$; $Q \neq 1$.

The straight line of Figure 6 can only be explained by Eq. (A11) if $(1 - Q)$ becomes very small. We assume $Q = 1$, i.e., $\varepsilon_A = \varepsilon_D$ and we will see later how far this assumption is necessary. The slopes and the intercept of the lines in Figure 6 are:

$$S = 2\,K_D(1+R)/\alpha^2 \quad \text{and} \quad I = \psi/\alpha\,. \tag{A15}$$

The slope is larger by a factor $(1 + R)$ than the slope in the BAB model.

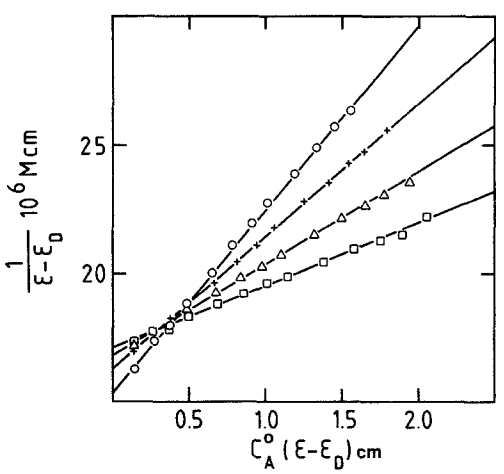

Fig. 6. The absorption measurements at 492 nm are plotted following Eq. (A12). The axis intercept I and the slope S can be determined at constant c_B. ○: $c_B = 0$ M; ×: $c_B = 0.003$ M; △: $c_B = 0.007$ M; □: $c_B = 0.015$ M

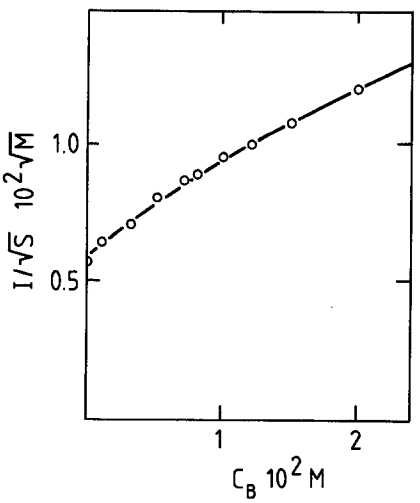

Fig. 7. The axis intercept I and the slope S determined in Figure 6 are plotted following Eq. (A14). The data points are fitted by the calculated curve

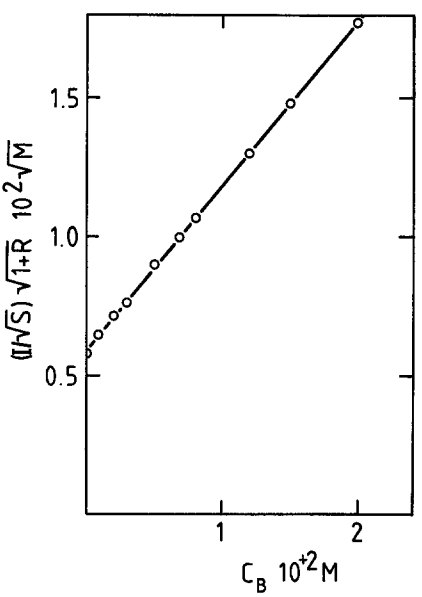

Fig. 8. The axis intercept I and the slope S determined in Figure 6 are plotted following Eq. (A16). The axis intercepts is $(2\ K_D)^{-1/2}$ and the slope $K_{AB}/(2\ K_D)^{1/2}$

The α is eliminated also by forming the ratio.

$$I/S^{1/2} = (1 + K_{AB}c_B)/[(2\ K_D)^{1/2}(1 + R)^{1/2}]\,. \tag{A16}$$

The slope in a plot of $I/S^{1/2}$ as a function of c_B would be decreasing (Fig. 7). A plot of $(I/S^{1/2})(1 + R)^{1/2}$ as a function of c_B should become a straight line for the correct K_A. Taking the correlation coefficient as a measure for the linearity of the plot, we found $R = 56.9\ \mathrm{M}^{-1}$ c_B to be the best value. The slope of the line is $K_{AB}/(2\ K_D)^{1/2}$ and the intercept $(2\ K_D)^{-1/2}$. From Figure 8 we found: $K_{AB} = 100 \pm 5\ \mathrm{M}^{-1}$ and $K_A = 8.2 \cdot 10^3\ \mathrm{M}^{-1}$ and from Eqs. (A15) and (A4)

$$\alpha = \psi/I\,,$$

$$\phi = (1/I + \varepsilon_D)\psi = \varepsilon_M + \varepsilon_{AB}K_{AB}c_B\,. \tag{A17}$$

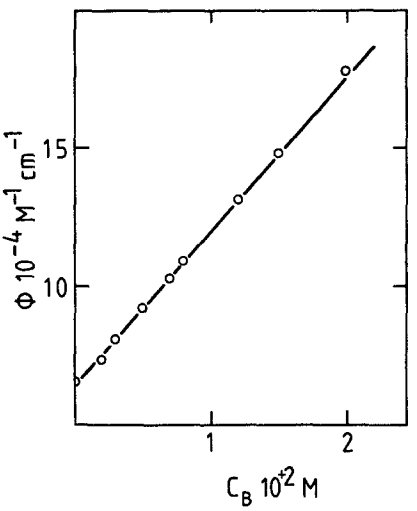

Fig. 9. ϕ calculated from Eq. (A17) as a function of c_B yields a straight line with the slope $K_{AB}\varepsilon_{AB}$. This determines ε_{AB}

A plot of ϕ as a function of c_B has a slope of $\varepsilon_{AB}K_{AB}$ and the intercept is ε_M. From Figure 9: $\varepsilon_{AB}^{492} = 5.5 \cdot 10^4\ M^{-1}$, $\varepsilon_M^{492} = 6.52 \cdot 10^4\ M^{-1}$.

The intercept ε_M is 2.5% smaller than determined with pure AO. With the measured data for any value of $\varepsilon_A < 5{,}000\ M^{-1}\ cm^{-1}$ no detectable change in the absorption measurements could be seen.

The results show that the complex BAB is not formed for 5′-AMP concentrations smaller than $2 \cdot 10^{-2}$ M. If in the AAB model some BAB complexes would have been present (K_B small but $K_B \neq 0$), values of K_{AB} and K_A would have been determined too small. Therefore the current values must be considered as lower limits. The AAB model fits the absorption data when $\varepsilon_A^{492} < 5{,}000\ M^{-1}\ cm^{-1}$. ε_A^{492} is of the same magnitude as ε_D^{492} and K_A the same as K_D. Therefore the assumption that the second AO binds to the AB on the A side is confirmed. This complex could also be formed by binding an AO dimer to the 5′-AMP, but the two mechanisms can only be discriminated by fast kinetics. We prefer the model of binding one AO after the other because it is more general and it is not known if the relative orientation of the two molecules remains the same as in the dimer.

References

Armstrong, R. W., Kurucsev, T., Strauss, U. P.: The interaction between acridine orange dyes and deoxyribonucleic acid. J. Am. Chem. Soc. **92,** 3174–3181 (1970)

Blake, R. D., Fresco, J. R.: Polynucleotides XI. Thermodynamics of $(A)_N \cdot 2\ (U)_\infty$ from the dependence of T_m on oligomer length. Biopolymers **12,** 775–789 (1973)

Bloomfield, V. A., Crothers, D. M., Tinoco, I.: Physical chemistry of nucleic acids. New York, N.Y.: Harper and Row 1974

Dourlent, M., Hélène, C.: A quantitative analysis of proflavine binding to polyadenylic acid, polyuridylic acid, and transfer RNA. Eur. J. Biochem. **23,** 86–95 (1971)

Eggimann, R.: Kooperative Komplexbildung von organischen Farbstoffen. Ph. D. Thesis, University of Basel (1974)

Evans, F. E., Sarma, R. H.: Intermolecular orientations of adenosine-5′-monophosphate in aqueous solution as studied by fast Fourier transform ^{1}H NMR spectroscopy. Biopolymers **13,** 2117–3132 (1974)

Halm, T. E., Ciak, J.: Progress in molecular and subcellular biology. Han, F. E. (ed.), vol. 2, p. 329. Berlin, Heidelberg, New York: Springer 1971

Imae, T., Ikeda, S.: Circular dichroism and structure of the complex of acridine orange with polyglutamic acid. Biopolymers **15,** 1655–1667 (1976)

Ising, E.: Beitrag zur Theorie des Ferromagnetismus. Z. Physik **31,** 253–258 (1925)
Kurucsev, T., Strauss, U. P.: Derivation and interpretation of the spectrum of the dimer of acridine orange hydrochloride, dilute aqueous solutions, and oriented film studies. J. Phys. Chem. **74,** 3081–3085 (1970)
Lamm, E., Neville, M.: The dimer spectrum of acridine orange hydrochloride. J. Phys. Chem. **69,** 3872–3877 (1965)
Lehninger, A. L.: Biochemistry. New York, N.Y.: Worth Publishing Inc. 1970
Lerman, L. S.: The structure of DNA-acridine complex. Proc. Natl. Acad. Sci. USA **49,** 94–102 (1963)
Menter, J. M., Hurst, R., West, S. S.: II. Binding constant and cooperativity parameters of acridine orange-dermatan sulfate system. Biopolymers **16,** 695–702 (1977)
Moroshkina, E. B., Shishov, A. K., Kirivtsova, M. A., Zhadin, N. N., Frisman, E. V.: Investigation of the influence of acridine dyes on the molecular structure of DNA. Mol. Biol. **9,** 668–674 (1976)
Pritchard, N. J., Blake, A., Peacocke, A. R.: Modified intercalation model for the interaction of amino acridines and DNA. Nature **212,** 1360–1361 (1966)
Robinson, B. H., Löffler, A., Schwarz, G.: Thermodynamic behaviour of acridine orange in solution. J. Chem. Soc. Faraday Trans I **69,** 56–69 (1973)
Schreiber, J. P., Daune, M. P.: Fluorescence of complexes of acridine dye with synthetic polydeoxyribonucleotides: A physical model of frameshift mutation. J. Mol. Biol. **83,** 487–501 (1974)
Schwarz, G.: Cooperative binding to linear biopolymers. 1. Fundamental static and dynamic properties. Eur. J. Biochem. **12,** 442–453 (1970)
Schwarz, G., Balthasar, W.: Cooperative binding to linear biopolymers. 3. Thermodynamic and kinetic analysis of the acridine orange-poly(L-glutamic acid)system. Eur. J. Biochem. **12,** 461–467 (1979)
Singer, M. F., Heppel, L. A., Ruskinzky, G. W., Sorber, H. A.: Spectral properties of adenine oligoribonucleotides. Biochim. Biophys. Acta **61,** 474–477 (1962)
Söderström, K. O., Parvinen, L. M., Parvinen, M.: Early detection of cell damage by supravital acridine orange staining. Experientia **33,** 265–266 (1977)
Taraganos, F., Darzynkiewicz, Z., Sharpless, T., Melamed, M. R.: Simultaneous staining of ribonucleic and deoxyribonucleic acids in unfixed cells using acridine orange in a flow cytofluorometric system. J. Histochem. Cytochem. **25,** 46–56 (1977)
Tomson, S. H.: Tumor destruction due to acridine orange photoactivation by argon laser. Ann. N.Y. Acad. Sci. **267,** 191–198 (1976)
West, S. S., Hurst, R. E., Menter, J. M.: Thermodynamics of mucopolysaccharide-dye binding. I. Identification of free and bound dye via membrane filtration: acridine orange-dermatan sulfate system. Biopolymers **16,** 685–693 (1977)
Zanker, V.: Über den Nachweis definierter reversibler Assoziate („reversible Polymerisate") des Acridinorange durch Absorptions- und Fluoreszenzmessungen in wäßriger Lösung. Z. Physik. Chem. **199,** 225–258 (1952)

Received July 5, 1978/Accepted November 7, 1978